Advances in Ultrasonic Monitoring of Oil-in-Water Emulsions

Valerie J Pinfield

Chemical Engineering Department, Loughborough University, Loughborough, LE11 3TU, UK

Email: v.pinfield@lboro.ac.uk Phone: +(44)1509 222512

Abstract

A modification to the multiple scattering model used to interpret ultrasonic measurements for emulsions is investigated. The new model is based on a development by Luppé, Conoir and Norris (2012) which accounts for the effects of multiple mode conversions between thermal, shear and compressional modes. The model is here applied to the case of oil in water emulsions in which thermal effects are dominant. The additional contributions are expressed in terms of the scattering coefficients for conversion between compressional and thermal modes and vice versa. These terms are due to the effect of thermal waves produced at one particle being reconverted into the compressional mode at neighboring particles. The effects are demonstrated by numerical simulations for a sunflower oil in water emulsion which show that the additional terms are significant at low frequency and high concentrations. Comparison is also made with experimental data for a hexadecane in water emulsion. Although qualitative agreement is demonstrated, there are some quantitative differences, which are attributed to uncertainties in the physical properties, in the experimental data, or in the assumptions made in the model.

Keywords: ultrasonic; emulsions; multiple scattering; thermal scattering

1 Introduction

Low-power non-destructive ultrasonic monitoring techniques have been successfully applied to a variety of hydrocolloid systems. The technique can be used for the measurement of concentration and particle size (Challis, Povey, Mather and Holmes, 2005, Babick, Stintz and Richter, 2006, McClements and Coupland, 1996), monitoring instability such as creaming/sedimentation (Pinfield, Povey and Dickinson, 1996) and flocculation (Chanamai and McClements, 2001, Herrmann, Hemar, Lemarechal and McClements, 2001), as well as for the detection of structural change such as gelation (Yuno-Ohta and Corredig, 2007, Audebrand, Kolb and Axelos, 2006) or crystallization (Coupland, 2002). One of the principal formulations for interpreting measurements is that based on a multiple scattering model, treating particles as independent scatterers of ultrasound, and combining the effects of scattering at each particle. Epstein and Carhart (1953) and Allegra and Hawley (1972) derived the solution for the scattering of a sound wave by a single spherical particle, taking into account both the thermal and shear waves produced in the process. Their results, combined with the multiple scattering model of Lloyd and Berry (1967) are here identified as the ECAH/LB model. This model is used to derive the effective wavenumber for ultrasound in emulsions or suspensions, from which the ultrasound speed and attenuation can be determined. The attenuation and speed depend on the physical properties of the component materials, and the particle size distribution (PSD) and concentration. By inverting the model using experimental measurements it is possible to determine PSD, concentration or certain properties by use of the ultrasonic technique. Ultrasonic measurements (of speed or attenuation) are typically carried out in through-transmission mode in the mega-Hertz frequency range which is ideally suited to applications in the colloidal size range. Ultrasonic techniques have some

advantages over other process analytical techniques for industrial applications, particularly in the fact that no dilution is necessary, and the equipment can be readily installed in a flow pipe.

The interpretation of measurements is an essential part of the technique, and so the existence of a valid model is crucial. Whilst the ECAH/LB model has been validated and used in a number of applications (see examples in Challis, Povey, Mather and Holmes, 2005), it is known to break down at low frequencies, high concentrations or small particle sizes. Evidence for the discrepancy between model and experiment can be found, for example in the work of Hipp (2002a-b) for silica in water suspensions and by McClements and others for oil in water emulsions (McClements, Hemar and Herrmann, 1999, Chanamai, Herrmann and McClements, 1999). The problem occurs when the thermal and shear waves produced at each particle by the scattering process, propagate a sufficient distance into the continuous phase that they can be re-scattered by a neighboring particle. This can result in a "reclaim" of the energy lost in these wave modes, so that the attenuation of the compressional mode (the transmitted mode of propagation) is reduced. The scattering model of ECAH/LB assumed that the thermal and shear wave modes decayed to zero in the space between particles and had no interaction with neighboring particles. This is a reasonable assumption in many cases, since the thermal and shear decay length is of the order of micrometers in water at 1 MHz. The magnitude of the "overlap" effect is governed by both the average interparticle distance, and the decay length of the thermal and shear wave modes (proportional to their wavelength). The effect becomes stronger at lower frequencies (where the decay length is longer), smaller particle size (where the interparticle distance is reduced at the same volume fraction of particles) and at higher concentrations (where the interparticle distance is reduced). Figure 1 illustrates the scattered compressional and thermal modes, which contribute to the wave field which is incident at a neighboring particle.

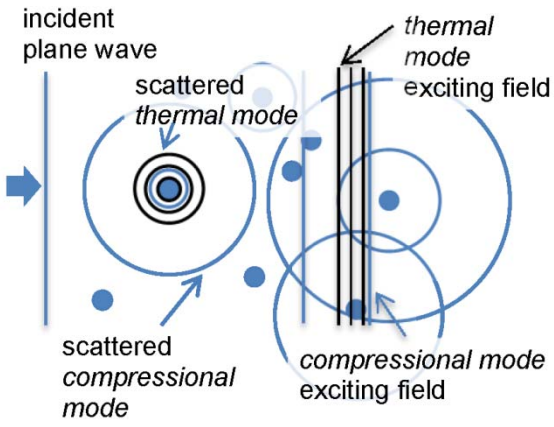

Figure 1 Illustration of the superposition of scattered waves of compressional and thermal modes for an incident compressional plane wave. The scattered waves combine to form a plane wave of each mode after averaging over particle locations.

The thermo-elastic effect which relates to the *thermal* scattering problem was solved by Isakovich (1948) for dilute emulsions by thermodynamic principles. A further extension to the result was published by Hemar, Herrmann, Lemaréchal , Hocquart and Lequeux (1997). Later, McClements, Hemar and Herrmann (1999) and Chanamai, Herrmann and McClements (1999) developed a core-shell model for the same system, including viscous effects and intrinsic absorption, and incorporated it into the existing ECAH/LB multiple scattering model. Hipp (2002a-b) also derived a core-shell model to account for both thermal and shear wave overlap effects within a multiple scattering model. These authors have demonstrated some success in matching theoretical predictions with experimental measurements for oil in water emulsions.

However, the core-shell model does suffer from some disadvantages. The most general form provided by Hipp requires numerical solution of 12x12 matrix equation which is numerically badly conditioned; such complexity is inappropriate for use embedded in an in-line monitoring system. The analytical version derived by the McClements groups is not readily applied to polydisperse systems and was extended beyond the long wavelength region by using a conversion factor applied to the more general scattering coefficient solution.

In this paper we present an alternative approach to the thermal multiple scattering problem (thermal overlap), based on a generalized multiple scattering model of Luppé, Conoir and Norris (2012). Luppé et al. (2012) extended the multiple scattering model of Waterman and Truell (1961), which is similar to that of Lloyd and Berry (1967), by including the combined scattered thermal and viscous wave fields which had previously been neglected. As illustrated in Figure 1, they considered the contribution of the scattered thermal and viscous waves to the wave field which is incident at a neighboring particle, and can be reconverted back into the compressional mode. Their mathematical result for the effective wavenumber has yet to be tested numerically and against experiment for typical colloidal and nanoparticle systems. The work reported here studies the contribution made by the additional thermal scattering terms which are significant for emulsions. The results of numerical calculations are compared with previously published experimental data.

2 Methods

2.1 Ultrasonic scattering theory

The three wave modes which are considered in the ECAH/LB formulation are the compressional, thermal and shear modes, with wavenumbers

$$k_C = \frac{\omega}{v} + i\alpha \qquad k_T = \left(\frac{\omega\rho C_p}{2\tau}\right)^{1/2}(1+i) \qquad k_S = \left(\frac{\omega\rho}{2\eta}\right)^{1/2}(1+i) \tag{1}$$

where k is a wavenumber, with subscripts C, T, S denoting the compressional, thermal and shear mode respectively. The angular frequency is ω and the speed and attenuation of the compressional mode are represented by v and α respectively. Physical properties of the material are denoted by ρ for the density, C_p for the heat capacity, τ for the thermal conductivity, and η for the shear viscosity; $i = \sqrt{-1}$. It can be seen from the wavenumber equations, that the thermal and shear wave modes have equal real and imaginary parts, so that they lose 1/*e* of their amplitude in a distance of $\lambda/2\pi$ where λ is the wavelength.

The scattering of an incident planar compressional wave by a single spherical particle was expressed by Epstein and Carhart (1953) and Allegra and Hawley (1972) as a sum of partial waves (spherical harmonics multiplied by radial dependence functions). Their scattering coefficients, denoted by A_n, B_n, C_n for the scattered compressional, thermal and shear wave modes respectively, are the amplitudes of the scattered partial waves for each mode. Their notation can be generalized to an incident wave of any mode by use of a "transition operator", $T_n^{qp}(\mathbf{r})$, which defines the transformation of the incident plane wave into scattered waves of any mode. For an incident wave of mode *q* which can be defined by a scalar potential Φ (compressional and thermal modes), the planar incident field is expressed as

$$\Phi_{0q} = \sum_{n=0}^{\infty} i^n (2n+1) j_n(k_q r) P_n(\cos\theta)$$

and the scattered fields of mode *p* by

$$\Phi_{0p} = \sum_{n=0}^{\infty} T_n^{qp} h_n(k_p r) P_n(\cos\theta)$$

where *p* and *q* can be any mode *C,T,S* (shear wave modes require a vector potential, not a scalar potential as written here). The scattered fields are written using spherical coordinates $\mathbf{r} = (r, \theta, \phi)$ with origin at the particle center, j_n and h_n are spherical Bessel and Hankel functions respectively, and P_n denotes the Legendre polynomials. Thus the transition operator $T_n^{qp}(\mathbf{r})$ defines the transformation from incident to scattered fields thus

$$T_n^{qp}(\mathbf{r}) j_n(k_q r) P_n(\cos\theta) = T_n^{qp} h_n(k_p r) P_n(\cos\theta)$$

The factors T_n^{qp} (not to be confused with the *operator* $T_n^{qp}(\mathbf{r})$) are equivalent to the scattering coefficients for the particular case of an incident compressional wave, for example, $T_n^{CT} = B_n$. The solution for the scattering factors (transition factors) for a *compressional* incident wave (*q*=*C*) was solved by Epstein and Carhart (1953) and Allegra and Hawley (1972) by considering the boundary conditions at the surface of the particle (continuity of displacement, temperature and heat flow, and stress conditions).

In order to determine the wavenumber for propagation of the compressional mode in an emulsion or suspension, containing many individual particles, a multiple scattering model is used. The most widely adopted is that of Lloyd and Berry (1967), although the same result has been obtained by Fikioris and Waterman (1964), building on their earlier work (Waterman and Truell, 1961). A new derivation of the same formula was reported by Linton and Martin (2006). The multiple scattering model considers the sum of all the scattered fields from all the individual particles, and averages over all possible locations for those particles. The resulting scattered field (for the compressional mode) combined with the incident (compressional) planar field is itself planar in nature, with a wavenumber which is defined as the effective wavenumber for propagation in the suspension/emulsion. This ensemble-averaged field is called the coherent field. The effective wavenumber for the compressional mode, K_C, can be written as a series expansion in the volume fraction, ϕ thus

$$\frac{K_{C,LB}^2}{k_C^2} = 1 - \frac{3i\phi}{k_C^3 a^3} \sum_{n=0}^{\infty} (2n+1) T_n^{CC} - \frac{27\phi^2}{k_C^6 a^6} \left(T_0^{CC} T_1^{CC} + \frac{10}{3} T_0^{CC} T_2^{CC} + 2\left(T_1^{CC}\right)^2 + 11 T_1^{CC} T_2^{CC} + \frac{230}{21}\left(T_2^{CC}\right)^2 + \ldots \right) \quad (2)$$

for a monodisperse system with particle radius a. The effective wavenumber has been given the additional subscript *LB* to denote the Lloyd and Berry solution. Here the second order terms in concentration are only shown up to the second partial wave order, which is valid for long wavelength applications where $k_C a \ll 1$ The scattering coefficients T_n^{CC} are often written A_n since only compressional coherent field was considered.

2.2 Multi-mode multiple scattering

Luppé, Conoir and Norris (2012) have recently extended the multiple scattering model to include the coherent fields resulting from the scattered thermal and shear wave modes as well as the compressional mode. The thermal and shear wave coherent fields contribute to the wave which is incident at any particle, and therefore, by mode conversion, produce scattered compressional waves. This results in a change to the coherent compressional mode (which is the result of the outgoing scattered compressional modes from all particles). They found additional contributions to the second order terms (in concentration) of the effective wavenumber for the compressional mode. Their result is expressed in terms of infinite sums over partial wave orders, with sums over all combinations of conversion between one mode and another, and includes the Gaunt coefficients to define the relationship between combinations of spherical harmonics. The result is not reproduced here due to its complexity, however, the work reported here is based on equations (29-32) of Luppé et al. (2012), which the authors term the "low concentration expansion" (a series in orders of volume fraction). Although we are still concerned with the effective wavenumber of the compressional mode, since in measurement we transmit and receive this mode, the additional terms derived by Luppé et al. (2012) represent the effects of multi-mode scattering. For example, the thermal waves produced at one particle are incident at a neighboring particle and can be converted partially back into the compressional mode, which contributes to the total compressional wave field.

2.3 Modification for thermal multiple scattering

2.3.1 Modification to multiple scattering

In order to the render the new multiple scattering model (Luppé et al., 2012) workable for a real measurement application, it is necessary to identify which of the new multi-mode scattering terms are significant in typical systems. As it stands, the effective wavenumber includes contributions from conversion of any mode into any other mode, for any partial wave order. Whilst it is already established that the Lloyd and Berry (1967) result (equation 2) can be terminated above order 2 in the long wavelength region, a similar criterion is not yet known for the multi-mode terms. The focus of this study was to develop a form of the new multi-mode scattering model which is applicable to oil in water emulsions. It has been demonstrated previously (Challis, Povey, Mather and Holmes, 2005) that for typical oil in water emulsions, the scattering of the compressional mode is dominated by conversion into the thermal mode, as well as the contributions due to compressibility difference. Hence, the effective wavenumber (equation 2) is dominated by the effects of the zero order coefficient T_0^{CC} which incorporates both of these contributions. Where the density of oil and water are reasonably closely matched, the contributions from the first order partial waves and higher terms can be neglected. This encapsulates the fact that conversion from compressional mode into shear mode is negligible in this case.

Building on this prior knowledge, the analysis of the new wavenumber which is reported here neglects any multi-mode scattering contributions from compressional-shear conversion or vice versa, and only includes compressional-thermal conversion and vice versa. In addition, since scattering of an incident compressional wave produces a significant amplitude of scattered thermal mode for the zero'th partial wave, only the zero order is considered. Finally, it is assumed that the conversion of an incident thermal wave will only produce significant conversion to scattered compressional modes for the zero partial wave order. In summary, then, the development is based on the following assumptions:

1. multi-mode scattering of the shear mode is neglected (scattered shear waves are assumed to have no effect on neighboring particles)

2. scattered thermal waves are only produced from the zero order partial wave of the incident compressional wave
3. scattered compressional waves produced by an incident thermal wave only result from the zero order partial wave

These assumptions reduce the complexity of the effective wavenumber expression considerably, and the remaining additional multi-mode contributions can be written as

$$\Delta\frac{K_C^2}{k_C^2}=-\frac{27\phi^2}{(k_c a)^6}\frac{k_c^3}{6k_T\left(k_c^2-k_T^2\right)}\left[(2ik_T a-1)j_0(k_c b)-(k_c b)j_0'(k_c b)\right]\cdot\left\{T_0^{CT}\cdot h_0(k_T a)\right\}\left\{\frac{T_0^{TC}}{j_0(k_T a)}\right\}\left(1-e^{2ik_T a}\right) \quad (3)$$

such that the effective wavenumber, now denoted $K_{C,LCN}$ is given by $K_{C,LCN}^2/k_C^2=K_{C,LB}^2/k_C^2+\Delta\left(K_C^2/k_C^2\right)$. The exclusion distance (the distance of closest approach between particle centers) is denoted *b* and subsequently taken as $b=2a$. It should be noted that the derivation does not make any assumptions on the magnitude of the thermal wavenumber-radius product $k_T a$. Under the assumptions made in the derivation, the two remaining scattering coefficients, or transition factors, are:

1. T_0^{CT} : the zero order partial wave amplitude of the thermal wave produced by an incident compressional wave, denoted in earlier works as B_0.
2. T_0^{TC} : the zero order partial wave amplitude of the compressional wave produced by an incident thermal wave.

These transition factors have been written in equation 3 in combination with the spherical Bessel and Hankel functions of the thermal wave number-radius product i.e. $\left\{T_0^{CT}\cdot h_0(k_T a)\right\}$and $\left\{T_0^{TC}/j_0(k_T a)\right\}$. This scaling is convenient for numerical stabilization of the calculations of the coefficients, as discussed by the author previously (Pinfield, 2007).

2.3.2 Scattering coefficient for incident thermal wave

Whilst the coefficient T_0^{CT} is produced directly from the matrix boundary equation solution for the compressional incident wave and was denoted B_n (ECAH model), the coefficient T_0^{TC} has not previously been derived as it was not needed for the previous multiple scattering models. This coefficient T_0^{TC} results from the scattering by a single spherical particle of an incident thermal wave, for the zero order partial wave mode. Since a thermal wave can be represented by a scalar potential in the same way as the compressional wave mode, the single-particle scattering solution follows that of Epstein and Carhart (1953) and Allegra and Hawley (1972) for the compressional incident wave. The main difference in this case, is that it is *not* assumed that $|k_T a|\ll 1$. Although the general solution of the boundary equations for incident compressional wave did not rely on the corresponding assumption $|k_C a|\ll 1$ for the compressional mode, some simplifications and analytical approximations did. These simplifications, therefore, cannot be adopted for the case of an incident thermal wave. A numerical solution for T_0^{TC} can be obtained from the same boundary matrix equation as used for the incident compressional wave solution, but replacing the incident wave, right-hand side terms with the corresponding terms for a thermal wave. See for example equation 9

of Challis, Povey, Mather and Holmes (2005), where all terms on the right hand side must be taken as functions of $k_T a$ rather than $k_C a$.

2.3.3 Calculations of new multi-mode scattering

Calculations have been carried out for the effective wavenumber for an oil in water emulsion, using the new multi-mode scattering formula, equations 2-3. Results are presented for the attenuation of a compressional wave through the emulsion. The compressional wave mode scattering coefficients T_n^{CC} were calculated from the matrix boundary equation in the usual way, up to and including order *n*=2. The additional coefficients needed for the extra thermal multi-mode contributions, T_0^{TC} and T_0^{CT} were also calculated using the matrix boundary equation, using compressional incident mode (for T_0^{CT}) and with thermal incident mode (for T_0^{TC}). Two systems were studied. Firstly, the trends for the additional contributions to attenuation are demonstrated using a monodisperse sunflower oil in water emulsion with a droplet radius of 0.1 μm and a temperature of 20 °C. The physical properties of the component fluids are shown in Table 1, after McClements and Povey (1989). Secondly, results for a hexadecane in water emulsion are presented, in comparison with experimental data published by McClements, Hemar and Herrmann (1999). Although hexadecane is not a food oil, the results serve to illustrate the typical contribution made by the additional thermal scattering terms for an oil in water system. These data were chosen because of the high quality and broad concentration and frequency range of the experimental data, although neither the physical properties used by the authors for their calculations nor the particle radius were stated in the paper (McClements et al. 1999). For the calculations presented here, the particle radius was taken to be 0.5 μm (monodisperse), the temperature 20 °C and the physical properties were taken from McClements and Coupland (1996), Table 1. These data provide a reasonable fit to the experimental data at low concentration (5%) where the additional thermal multi-mode scattering is not significant. Calculations were carried out using MATLAB®.

	Sunflower oil in water emulsion[a]		Hexadecane in water emulsion[b]	
	Water	Sunflower oil	Water	Hexadecane
Sound velocity / m s^{-1}	1482.3	1469.9	1485.5	1357.9
Density / kg m^{-3}	998.2	920.6	999.5	773.0
Shear viscosity / Pa s	0.001	0.054	0.00111	0.00334
Thermal conductivity / J $m^{-1}s^{-1}K^{-1}$	0.591	0.17	0.59	0.14
Heat Capacity C_p / J kg^{-1} K^{-1}	4182	1980	4182	2093
Expansivity / K^{-1}	0.00021	0.00071	0.000222	0.00091
Attenuation factor *y* /Np m^{-1} MHz^{-z}	0.026	1.15	0.025	0.101
Attenuation exponent *z*	2	1.77	2	2

[a] McClements and Povey (1989)

[b] McClements and Coupland (1996)

Table 1 Physical properties for the emulsions used for simulations. The attenuation is defined as a function of frequency *f* by the power law relationship $(\alpha/\mathrm{Np\,m^{-1}}) = (y/\mathrm{Np\,m^{-1}MHz^{-z}})(f/\mathrm{MHz})^z$. The two parameters *y* and *z* are given in the table.

3 Results and discussion

3.1 Behavior of new terms

The effects of multi-mode scattering are expected to be observed under conditions such that the thermal waves produced at one particle have not decayed sufficiently before reaching neighboring particles, and

can thus be re-scattered and converted back into the compressional mode. The decay length of the thermal waves can be written as

$$\delta_T \approx 1/\mathrm{Re}(k_T) = \frac{\lambda}{2\pi} = \sqrt{\frac{\tau}{\pi\rho C_p f}}$$

(see equation 1). This is the distance over which the amplitude of a thermal wave decays to 1/*e*. The average distance between particles of the emulsion can be approximated by

$$\delta \approx a\left(\phi^{-1/3} - 1\right)$$

Hence, thermal multi-mode scattering may be expected to be significant when the interparticle separation is of the order of the thermal decay length

$$\delta \leq \delta_T \qquad (4)$$

Since the decay length scales with the inverse of the square root of the frequency, it is expected that the effect will be insignificant at high frequencies, since the thermal waves have died away before reaching neighboring particles. At low frequencies, however, where the thermal decay length is large, the contribution from thermal multi-mode scattering is most significant, since the thermal waves create a significant incident field at neighboring particles. Similarly, at high concentrations, the average distance between particles is smaller, and thermal multi-mode scattering is again significant.

Figure 2 shows the attenuation as a function of frequency for the sunflower oil in water emulsion at 30% (by volume) predicted by the standard multiple scattering model, and the multi-mode scattering model, with the additional terms shown in equation 3. At the highest frequency range, the two models converge, demonstrating that the thermal multiple scattering contribution is negligible in this region, as expected. At lower frequencies, the attenuation is reduced by including the thermal mode conversion contributions. Energy is reclaimed from the scattered thermal wave field, and rescattered into the compressional mode, effectively reducing the overall energy lost from the transmitted compressional wave. On this logarithmic attenuation scale, the models diverge as frequency decreases, demonstrating that the thermal overlap effect is more significant at lower frequencies. In fact, the knee of the curve is the region where thermal scattering is at makes its greatest contribution to K_C^2/k_C^2, both the conversion of the compressional mode into thermal scattered waves, and the re-scattering contribution (equation 3) from mode re-conversion. This corresponds to the condition $\mathrm{Re}(k_T a) \approx 1$. However, the intrinsic attenuation increases strongly with frequency, so that the multi-mode model appears to make a more significant difference at low frequencies. Here, the thermal condition $\delta \approx \delta_T$ occurs at a frequency of 18.5 MHz, which corresponds to the convergence of the models (on this logarithmic scale at least) on Figure 2.

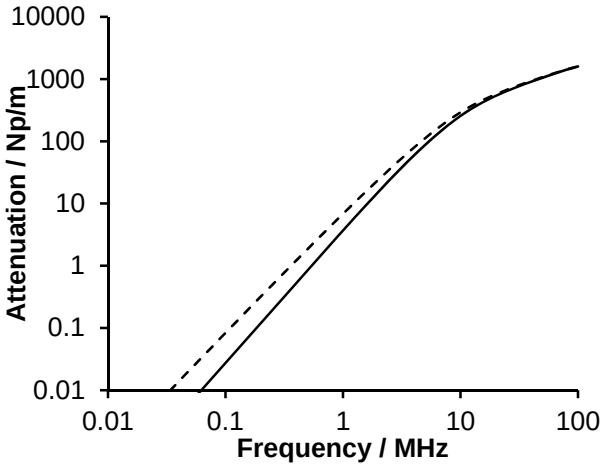

Figure 2 Predicted attenuation as a function of frequency for a 30% v/v monodisperse sunflower oil in water emulsion, with particle radius 0.1 μm, according to the Lloyd and Berry model (equation 2, dashed line) and the multi-mode scattering model (equation 3, solid line).

The trend of the additional contribution to attenuation with frequency and concentration is further explored in Figure 3 and Figure 4 for the sunflower oil in water emulsion. Figure 3 shows clearly that the reduction in attenuation due to the additional terms is strongest at the highest concentrations. As the concentration increases, the average interparticle separation is reduced, so that scattered thermal waves are more likely to reach neighboring particles and be converted back to the compressional mode. The results here are plotted on a linear frequency and attenuation scale, and the convergence of the models at high frequencies is not seen in this limited range. The effects of the thermal multi-mode scattering contribution are felt over a broad frequency range. Figure 4 shows clearly the divergence of the models as concentration increases, but in this case, a similar proportional contribution to attenuation is seen at all frequencies in the simulated range.

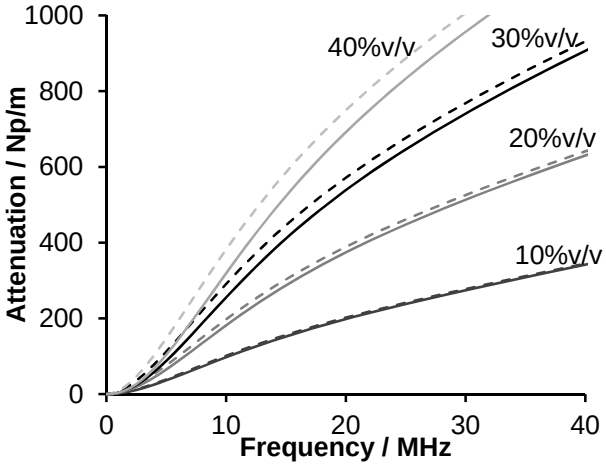

Figure 3 Predicted attenuation as a function of frequency for a 30% v/v monodisperse sunflower oil in water emulsion with particle radius 0.1 μm, for range of concentrations. Results are shown for the Lloyd and Berry model (equation 2, dashed lines) and the multi-mode scattering model (equation 3, solid lines).

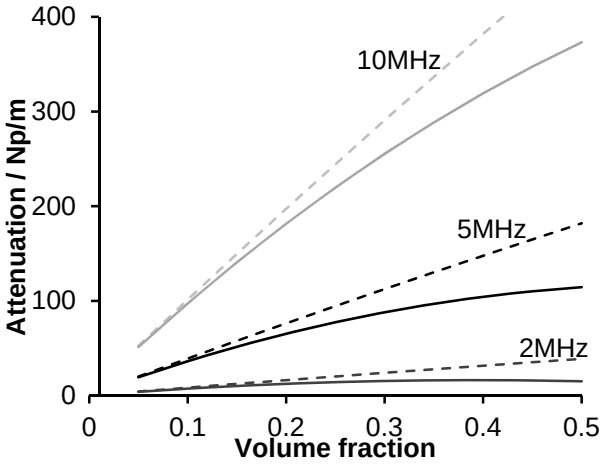

Figure 4 Predicted attenuation as a function of volume fraction for a 30% v/v monodisperse sunflower oil in water emulsion with particle radius 0.1 μm, for selected frequencies. Results are shown for the Lloyd and Berry model (equation 2, dashed lines) and the multi-mode scattering model (equation 3, solid lines).

In summary, then, the results of these simulated attenuation data have shown that the thermal multi-mode scattering makes a more significant contribution at lower frequencies, and at higher concentrations. This is consistent with a "thermal overlap" description, which considers the relative magnitude of the thermal mode decay length and the interparticle separation. The results are an encouraging test of the model, which demonstrate that it behaves as expected in terms of attenuation reduction due to thermal re-conversion into the compressional mode.

3.2 Comparison with experiment

To compare the model with experimental data, data for the measured attenuation for a monodisperse hexadecane in water emulsion, reported by McClements, Hemar and Herrmann (1999), are used (Figure 5). The data is plotted as excess attenuation (total attenuation minus the volume-averaged attenuation of the two component phases) per wavelength (of water), $\Delta\alpha \cdot \lambda$, as a function of the product of frequency and the square of particle radius, fa^2. This scaling is known to be valid for the scattering processes, which scale with fa^2 through thewavenumber-radius product $k_T a$. Although McClements et al. (1999) present a large number of experimental data points, only a few selected points are shown here to illustrate the trend of the experimental results.

At 5% concentration by volume (Figure 5a) the Lloyd and Berry model, and the multi-mode model are indistinguishable, since thermal multi-mode scattering is negligible at this concentration. The simulated data agrees reasonably well with experiment, although the simulation overestimates attenuation at the higher frequencies slightly. Figure 5b-e show that the attenuation reduction due to multi-mode scattering is only significant below the peak of the curves and slightly beyond it, and is stronger as the concentration increases, as observed previously. At the higher frequencies, at all concentrations, the two models agree. The multi-mode scattering contributions do not appear to provide sufficient reduction in attenuation above the peak of the curve where the attenuation is overestimated for both models compared with the experimental data. The experimental data at frequencies below the peak of the curve, fall below that predicted by the Lloyd and Berry model, so the additional scattering contributions act in the right direction to improve the agreement between model and experiment. At 20% v/v (Figure 5c), for example, the multi-mode scattering model does appear to produce an improved fit to experiment in the lower frequency part of the curve, although there is some variation in the experimental data. However, at higher concentrations,

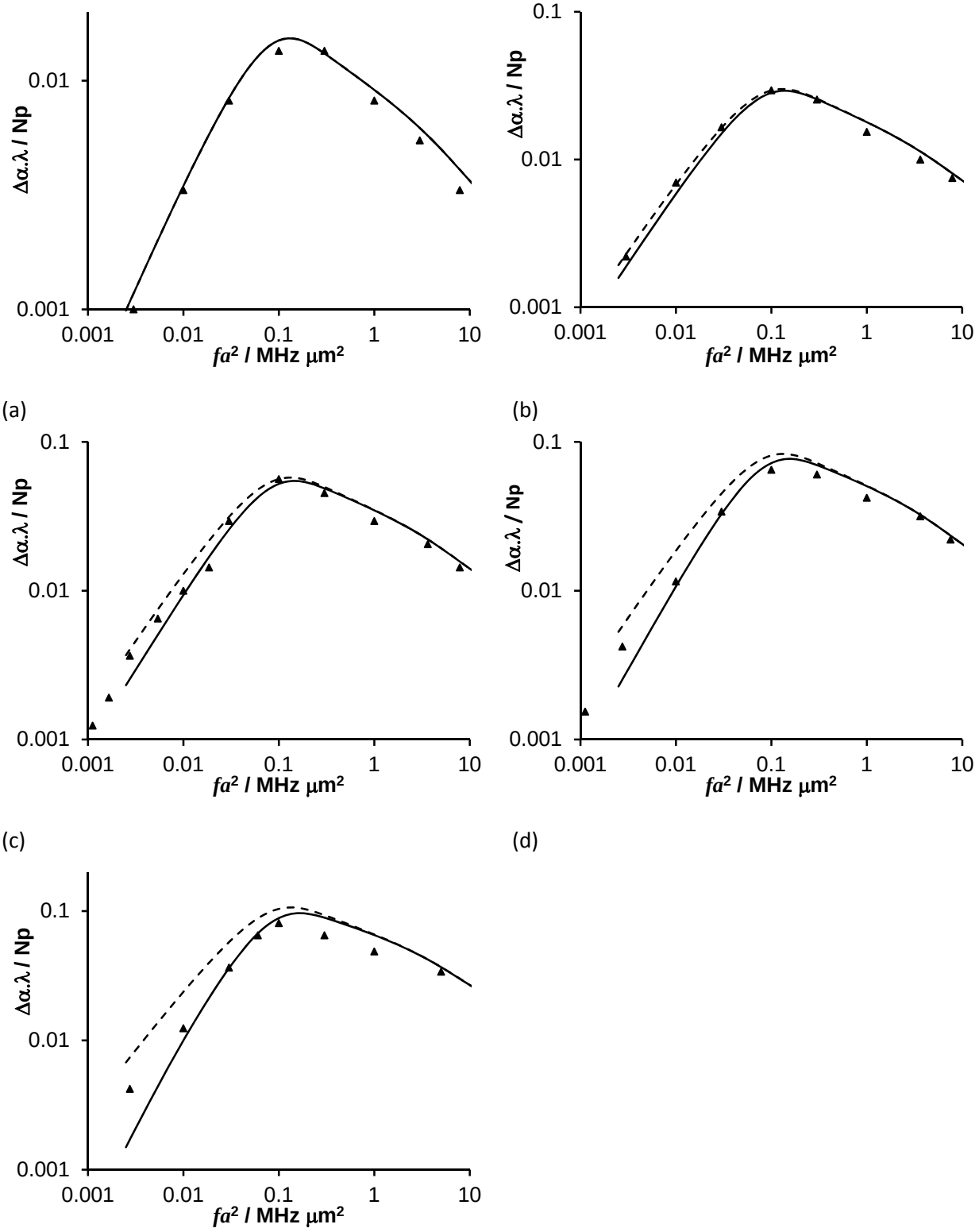

Figure 5 Excess attenuation per wavelength ($\Delta\alpha \cdot \lambda$) as a function of frequency multiplied by the square of particle radius (fa^2) for monodisperse hexadecane in water with radius 0.5 μm. Results are shown for the Lloyd and Berry model (equation 2, dashed lines) and the multi-mode scattering model (equation 3, solid lines) at different concentrations (a) 5% v/v (b) 10%v/v (c) 20% v/v (d) 30% v/v (e) 40% v/v. Experimental data from McClements, Hemar and Herrmann (1999) are shown by triangles; only a small fraction of the experimental data presented by the authors are shown here.

as shown in Figure 5d-e, the reduction in attenuation from multi-mode contributions at the lowest frequencies seems to be too great, and causes the attenuation to be underestimated. In fact the experimental data at these two highest concentrations (30% v/v and 40% v/v) are quite similar, and the difference in attenuation between them is small. The core-shell model used by McClements, Hemar and Herrmann (1999) to compare with this experimental data produced a better fit to the data than does the new model proposed here in its present form. However, the physical properties and particle radius used in their calculations were not stated, and hence remain uncertain in our present calculations.

3.3 Uncertainties

The results discussed in the two previous sections have demonstrated good qualitative trends, but not definitive quantitative agreement with experimental data. Based on this data, there seem to be two areas in which the multi-mode scattering model may not be accurate. Firstly, it appears to produce too strong a reduction in attenuation at the lowest frequencies (Figure 2Figure 5); this can be seen in the gradient of the curve towards the low frequency limit, which is steeper at the highest concentrations than the experimental data appears to be. Secondly, the multi-mode model does not reduce the attenuation sufficiently at frequencies above the peak of the curve. This can be seen by the convergence of the Lloyd and Berry and multi-mode models close to the peak in Figure 5, whereas the experimental data is lower than both models at higher frequencies.

There are a number of uncertainties in the comparison of simulation with experiment. Firstly, the material properties are not fully characterized – the physical properties were taken from an earlier paper, and the particle size was assumed (the chosen axis scaling should produce the same curve for all particle sizes within the long wavelength region). In addition, since the measured attenuation for the higher concentrations was very similar, it is difficult to distinguish model trends from experimental error. Figure 5a shows that at 5% v/v where the new thermal terms are insignificant, even the Lloyd and Berry model overestimates attenuation in this region. This suggests that the discrepancy at least above the peak of the curve may be due to uncertainty in the physical properties rather than due to inaccuracy in the new model.

A potentially more significant uncertainty lies within the model development itself. It was assumed that the only significant partial wave mode which contributes to the multi-mode scatter is the zero order mode. Although it is already known that the conversion from compressional mode into thermal mode is dominated by the zero order partial wave, the assumption that the same is true for the opposite conversion (incident thermal wave) is not underpinned by strong evidence thus far. A significant consideration may be that the thermal wavelength is not necessary large compared with the particle radius, which suggests that higher order partial waves may also contribute in the case of a thermal incident wave. Further numerical and analytical investigation is necessary to explore the magnitude of the higher order scattering coefficients, and also to identify how they contribute to the effective wavenumber. At this stage, only the zero order partial wave terms were identified in the effective wavenumber formulation (equation 3). The contribution from additional terms would need to be identified from the Luppé, Conoir and Norris (2012) formula for effective wavenumber. There is evidence from the numerical calculations that the additional thermal multi-mode scatter contributions are too large under some conditions (particularly at low frequency and high concentration), such that the effective wavenumber may take an unphysical value. This suggests that there are some contributions which have not been included in the model which become significant under these conditions, possibly reducing the magnitude of the additional contributions.

4 Conclusions

A modification to the multiple scattering model used for calculating attenuation (and speed) of compressional ultrasonic waves through emulsions has been presented. The result is a development of the work of Luppé, Conoir and Norris (2012) and identifies the most significant contribution due to thermal multi-mode scattering, arising from the zero order partial wave mode. New scattering coefficients have been calculated for the scattering of a thermal incident wave by a single spherical particle to determine the conversion into the compressional mode. Simulated attenuation spectra using the modified scattering model have been compared with the previous model for a sunflower oil in water emulsion. The results show that the model predicts a reduction in attenuation due to thermal mode conversion, which is most significant at low frequencies, and high concentration. This is consistent with the description of multi-mode scattering in terms of the decay of the scattered thermal waves in the space between particles. When particles are close together (at high concentrations), or when the decay length for the thermal waves is long (at low frequency) the thermal waves scattered by one particle can interact with neighboring particles, and can be converted to produce compressional waves.

The comparison of the model results with experimental data (McClements, Hemar and Herrmann, 1999) was qualitatively encouraging, but quantitatively not definitive. The trends of the model were consistent with the experimental data, but the reduction in attenuation in the model at low frequency appeared to be too strong, and at higher frequency too weak. However, uncertainties remain in the characterization of the experimental system, and a further experimental study is required to validate the model results. As it stands, the model reported here looks less successful in matching experimental results than the previous core-shell model (McClements et al., 1999), but given the uncertainties involved in the experimental comparison this may not be a generally applicable conclusion.

Further development of the model is required to investigate the assumptions made in its development, particularly in the selection of the single dominant contribution to the thermal multi-mode scattering, arising from the zero order partial wave mode. Future work will address the potential contributions from other partial wave modes, and calculate their effect on attenuation.

Acknowledgements

Prof Eric Dickinson was co-supervisor for my PhD studies in the 1990s, together with Prof Malcolm Povey. Eric has greatly influenced the way I approach scientific research; he had the wisdom to suggest and direct potential research paths whilst allowing me the freedom to develop my own research interests, and was at the same time challenging and encouraging. He has an impressive ability to comprehend the broad sweep of his chosen field, whilst also demonstrating an incredible depth of knowledge. I am indebted to him and delighted to contribute to this volume in his honor.

References

Allegra, J. R., & Hawley, S. A. (1972). Attenuation of sound in suspensions and emulsions: Theory and experiments. *Journal of the Acoustical Society of America, 51*, 1545-1564.

Audebrand, M., Kolb, M., & Axelos, M. A. V. (2006). Combined rheological and ultrasonic study of alginate and pectin gels near the sol-gel transition. *Biomacromolecules, 7*(10), 2811-2817.

Babick, F., Stintz, M., & Richter, A. (2006). Ultrasonic particle sizing of disperse systems with partly unknown properties. *Particle and Particle Systems Characterization, 23*, 175-183; 175.

Challis, R. E., Povey, M. J. W., Mather, M. L., & Holmes, A. K. (2005). Ultrasound techniques for characterizing colloidal dispersions. *Reports on Progress in Physics, 68*(7), 1541-1637.

Chanamai, R., Herrmann, N., & McClements, D. J. (1999). Influence of thermal overlap effects on the ultrasonic attenuation spectra of polydisperse oil in water emulsions. *Langmuir, 15*, 3418-3423; 3418.

Chanamai, R., & McClements, D. J. (2001). Depletion flocculation of beverage emulsions by gum arabic and modified starch. *Journal of Food Science, 66*(3), 457-463.

Coupland, J. N. (2002). Crystallization in emulsions. *Current Opinion in Colloid & Interface Science, 7*(5-6), 445-450.

Epstein, P. S., & Carhart, R. R. (1953). The absorption of sound in suspensions and emulsions. I. water fog in air. *Journal of the Acoustical Society of America, 25*(3), 553-565.

Fikioris, J. G., & Waterman, P. C. (1964). Multiple scattering of waves II. "hole corrections" in the scalar case. *Journal of Mathematical Physics, 5*, 1413-1420.

Hemar, Y., Herrmann, N., Lemarechal, P., Hocquart, R., & Lequeux, F. (1997). Effective medium model for ultrasonic attenuation due to the thermo-elastic effect in concentrated emulsions. *Journal De Physique II France, 7*, 637-647.

Herrmann, N., Hemar, Y., Lemarechal, P., & McClements, D. J. (2001). Probing particle-particle interactions in flocculated oil-in-water emulsions using ultrasonic attenuation spectrometry. *European Physical Journal E, 5*(2), 183-188.

Hipp, A. K., Storti, G., & Morbidelli, M. (2002). Acoustic characterization of concentrated suspensions and emulsions 1. model analysis. *Langmuir, 18*, 391-404; 391.

Hipp, A. K., Storti, G., & Morbidelli, M. (2002). Acoustic characterization of concentrated suspensions and emulsions 2. experimental validation. *Langmuir, 18*, 405-412; 405.

Isakovich, M. A. (1948). Op rasprostranenii zvuka v emulsiyakh. *Zhurnal Eksperimentalnoi I Teoreticheskoi Fiziki, 18*(10), 907-912.

Linton, C. M., & Martin, P. A. (2006). Multiple scattering by multiple spheres: A new proof of the lloyd-berry formula for the effective wavenumber. *Siam Journal on Applied Mathematics, 66*(5), 1649-1668.

Lloyd, P., & Berry, M. V. (1967). Wave propagation through an assembly of spheres IV relations between different multiple scattering theories. *Proceedings of the Physical Society, London, 91*, 678-688.

Luppé, F., Conoir, J. M., & Norris, A. N. (2012). Effective wave numbers for thermo-viscoelastic media containing random configurations of spherical scatterers. *Journal of the Acoustical Society of America, 131*(2), 1113-1120.

McClements, D. J., & Coupland, J. N. (1996). Theory of droplet size distribution measurements in emulsions using ultrasonic spectroscopy. *Colloids and Surfaces A: Physicochemical and Engineering Aspects, 117*, 161-170.

McClements, D. J., Hemar, Y., & Herrmann, N. (1999). Incorporation of thermal overlap effects into multiple scattering theory. *Journal of the Acoustical Society of America, 105*(2), 915-918.

McClements, D. J., & Povey, M. J. W. (1989). Scattering of ultrasound by emulsions. *Journal of Physics D: Applied Physics, 22*, 38-47; 38.

Pinfield, V. J. (2007). Acoustic scattering in dispersions: Improvements in the calculation of single particle scattering coefficients. *Journal of the Acoustical Society of America, 122*(1), 205-221; 205.

Pinfield, V. J., Povey, M. J. W., & Dickinson, E. (1996). Interpretation of ultrasound velocity creaming profiles. *Ultrasonics, 34*(6), 695-698.

Waterman, P. C., & Truell, R. (1961). Multiple scattering of waves. *Journal of Mathematical Physics, 2*, 512-537.

Yuno-Ohta, N., & Corredig, M. (2007). Characterization of beta-lactoglobulin A gelation in the presence of sodium caprate by ultrasound spectroscopy and electron microscopy. *Biomacromolecules, 8*(8), 2542-2548.

Figure Captions

Figure 1 Illustration of the superposition of scattered waves of compressional and thermal modes for an incident compressional plane wave. The scattered waves combine to form a plane wave of each mode after averaging over particle locations.

Figure 2 Predicted attenuation as a function of frequency for a 30% v/v monodisperse sunflower oil in water emulsion, with particle radius 0.1 μm, according to the Lloyd and Berry model (equation 2, dashed line) and the multi-mode scattering model (equation 3, solid line).

Figure 3 Predicted attenuation as a function of frequency for a 30% v/v monodisperse sunflower oil in water emulsion with particle radius 0.1 μm, for range of concentrations. Results are shown for the Lloyd and Berry model (equation 2, dashed lines) and the multi-mode scattering model (equation 3, solid lines).

Figure 4 Predicted attenuation as a function of volume fraction for a 30% v/v monodisperse sunflower oil in water emulsion with particle radius 0.1 μm, for selected frequencies. Results are shown for the Lloyd and Berry model (equation 2, dashed lines) and the multi-mode scattering model (equation 3, solid lines).

Figure 5 Excess attenuation per wavelength ($\Delta\alpha \cdot \lambda$) as a function of frequency multiplied by the square of particle radius (fa^2) for monodisperse hexadecane in water with radius 0.5 μm. Results are shown for the Lloyd and Berry model (equation 2, dashed lines) and the multi-mode scattering model (equation 3, solid lines) at different concentrations (a) 5% v/v (b) 10%v/v (c) 20% v/v (d) 30% v/v (e) 40% v/v. Experimental data from McClements, Hemar and Herrmann (1999) are shown by triangles; only a small fraction of the experimental data presented by the authors are shown here.